Catalytic ozonation of the antibiotic sulfadiazine: reaction kinetics and transformation mechanisms

Kråkström, Matilda; Saeid, Soudabeh; Tolvanen, Pasi; Salmi, Tapio; Eklund, Patrik Christoffer; Kronberg, Leif

Published in:
Chemosphere

DOI:
10.1016/j.chemosphere.2020.125853

Published: 01/05/2020

Document Version
Accepted author manuscript

Document License
CC BY-NC-ND

Catalytic ozonation of the antibiotic sulfadiazine: reaction kinetics and transformation mechanisms

Matilda Kråkström,*[a] Soudabeh Saeid,[b] Pasi Tolvanen,[b] Tapio Salmi,[b] Patrik Eklund,[a] Leif Kronberg[a]

* Corresponding author. Matilda.krakstrom@abo.fi, +358405574159

[a] Laboratory of Organic Chemistry, Johan Gadolin Process Chemistry Centre, Åbo Akademi University, Turku, Finland

[b] Laboratory of Industrial Chemistry and Reaction Engineering, Johan Gadolin Process Chemistry Centre, Åbo Akademi University, Turku, Finland

Declarations of interest: none

Keywords: ozonation, antibiotics, transformation product, mass spectrometry

Highlights

- The antibiotic sulfadiazine (SDZ) can be removed by ozonation
- The main transformation products were identified and quantified
- The removal of SDZ and its transformation products was compared for catalytic and non-catalytic ozonation
- A novel SDZ transformation pathway was investigated

Abbreviations

2-AP 2-aminopyrimidine

ESI Electrospray ionization

DCF diclofenac

IBU ibuprofen

MRM multiple-reaction-monitoring

SDZ Sulfadiazine

Abstract

In this work, ozone has been used to study the transformation of the antibiotic sulfadiazine (SDZ). SDZ and its transformation products was investigated using liquid chromatography coupled to mass spectrometry and using NMR. The results revealed that 6 % of SDZ is transformed into 2-aminopyrimidine. A significant amount of SDZ undergoes a rearrangement reaction followed by ring-closing reactions. One of these products, SDZ-P15, is the main product after 240 minutes of ozonation. Almost 30 % of SDZ transforms into SDZ-P15. SDZ was also transformed via the addition of one or more hydroxyl groups, via the oxidation of an amine group to a nitro group as well as via a bond cleavage reaction. Most of the intermediate products presented in this study have not previously been reported as SDZ transformation products formed using ozonation technology.

Acknowledgements

This work is a part of the acivities of the Johan Gadolin Process Chemistry Åbo Akademi University. Financial support from Svenska Litteratursällskapet (SLS), Vicotriastiftelsen, Stiftelsen för Åbo Akademi and maa- ja vesitekniikan tuki is gratefully acknowledged.

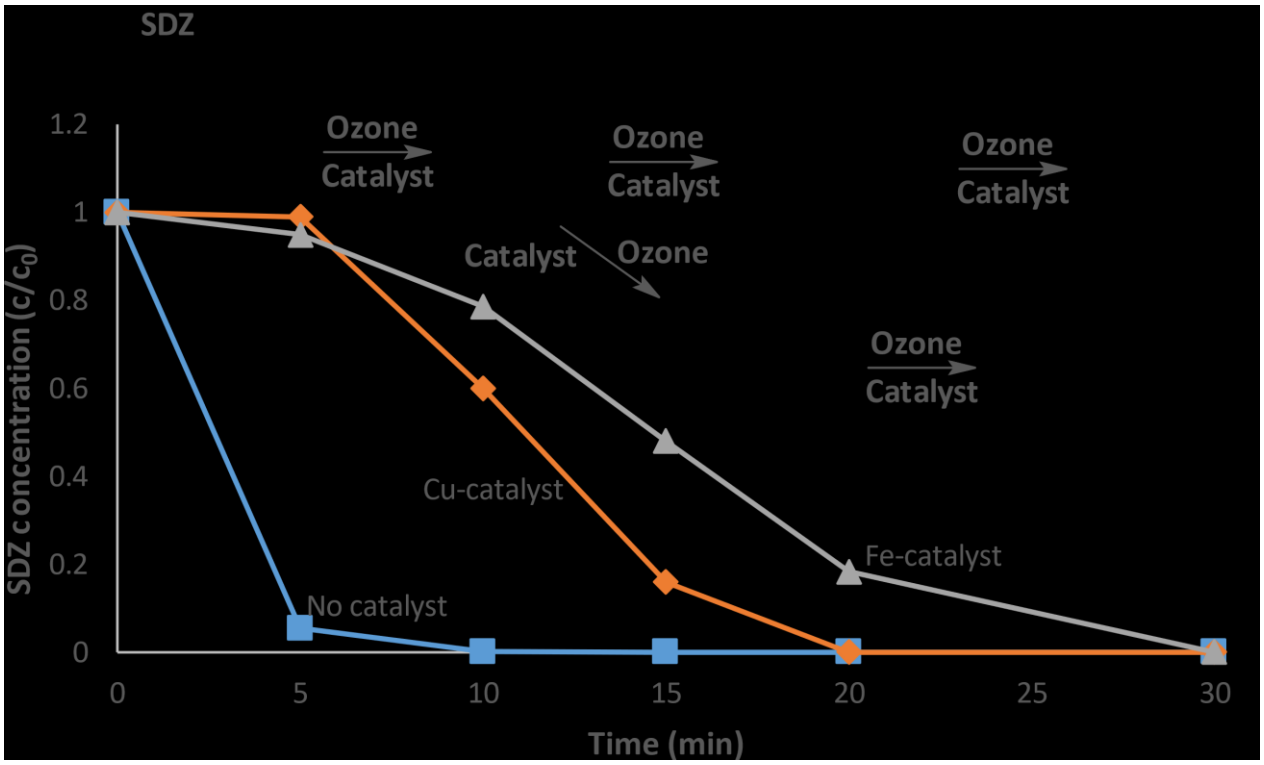
SDZ
1.2
1
0.8
0.6
0.4
0.2
0
SDZ concentration (c/c0)
Ozone
Catalyst
Ozone
Catalyst
Ozone
Catalyst
Catalyst
Ozone
Ozone
Catalyst
Cu-catalyst
Fe-catalyst
No catalyst
0
5
10
15
20
25
30
Time (min)

39

40

1. Introduction

Antibiotic resistance has been found to be present in the environment (Kümmerer et al. 2004; Witte 1998) due to the extensive use of antibiotics for both human and veterinary purposes (Witte et al. 1998). While the precise mechanism behind the emerging resistance is not yet understood it has been demonstrated that low, stable concentration levels of antibiotics favour the transfer of resistance genes (Kümmerer et al. 2004; Baquero et al. 2008). This could lead to the rise of resistance in the environment in the vicinity of wastewater treatment plants because low concentrations of antibiotics are continually released. In addition to the rise of antibiotic resistance, sulfonamide antibiotics inhibit the growth of plants (mi et al. 2009).

The sulfonamide antibiotic sulfadiazine (SDZ) has been detected in concentrations of up to 50 µg/L in wastewater influents (Michael et al. 2013) and 0.5 µg/L in wastewater effluents (Hong et al. 2008). Pharmaceuticals enter the environment mainly via domestic wastewater treatment plants (Pal et al. 2010; Li et al. 2014). SDZ concentrations of up to 66 ng/L have been detected in a Finnish river (Meierjohann et al. 2017) and 1 µg/L in Chinese river (Wei et al. 2010). Traditional wastewater treatment plants use only physical and biological treatment methods (Fatta-Kassinos et al. 2011) which are unable to remove organic compounds such as sulfadiazine completely. Thus, new treatment methods that are capable of removing sulfadiazine more efficiently are needed.

One popular oxidation technology applied on water treatment is ozonation. Sulfadiazine can be removed using this process (Garoma et al. 2010; Li et al. 2018), however, it is not completely mineralized in advanced oxidation processes (Rong et al. 2014; Fabiańska et al. 2014; Ma et al. 2015). Instead, it is transformed into different oxidation products. The transformation of pharmaceuticals and their products can be enhanced by combining ozonation with catalysis (Nawrocki et al. 2010). Catalysts used in combination with ozonation can be either homogenous or heterogenous. The advantage of

heterogenous catalyst is the easy separation of the catalyst from the liquid and the possibility to reuse the catalyst (Gomes et al. 2017).

Most commonly, ozonation reactions involve the reaction of hydroxyl radicals (Fatta-Kassinos et al. 2011). Typical reactions involve the addition of OH groups to aromatic rings, cleavage of C-O, C-N or S-N bonds, cleavage on α-position from the aromatic moiety and ring opening (Kosjek et al. 2008). Some pharmaceuticals, such as carbamazepine, undergo ring-closing reactions (McDowell et al. 2005).

It is important not only to study the disappearance of a reactant in the treatment process, but also to investigate which products are formed during the treatment. The reason for this is that the products might still be biologically active and in some cases, they might even be more toxic than the parent compound (Wang et al. 2018; Donner et al. 2013). For example, when the sulfonamide antibiotic sulfamethoxazole is treated with UV, the products formed are more toxic towards *D. magna* than the initial compound (Nasuhoglu et al. 2011). This implies that new wastewater treatment methods should be able not only to remove pharmaceuticals but also all the toxic transformation products which are formed during the oxidation process.

The fate of sulfadiazine in oxidation processes has been investigated; however, few studies have been conducted on the transformations that take place when SDZ is ozonated. The transformation of sulfadiazine involves complex reactions and the complete transformation pathway of sulfadiazine in oxidation processes has not yet been elucidated. Previous articles have published the rearrangement product which is formed when SDZ is oxidized (Neafsey et al. 2010; Wang et al. 2010; Gao et al. 2012; Zhou et al. 2016; Yang et al. 2017; Zou et al. 2014; Boreen et al. 2005; Yang et al. 2012), however the transformation product of this product have not previously been published. No studies have investigated how the presence of a solid catalyst affects the transformation products formed during ozonation. In previous studies, the identity of transformation products is based mainly on the data acquired by LC-MS

analyses and on the observed molecular weight of product peaks. In depth analysis of the acquired data is often lacking, resulting in the identification of only a few products and sometimes even misidentification of some products. In this work, we aim to more in depth study of transformation products. We have acquired not only the molecular weight of the products but further fragmentation pattens, in many cases high resolution MS data and finally provided by application of organic chemistry reaction mechanims, sound proposals on the pathway of formation of the products.

2. Methods

2.1. Chemicals and reagents

The internal standard, sulfadiazine-D4 was purchased from Toronto Research Chemicals, North York, ON, Canada. Analytical standard of sulfadiazine was purchased from Sigma-Aldrich (St. Louis, MO, USA) and 2-aminopyrimidine (98 % purity) was purchased from Acros organics (Geel, Gelgium). Stock solutions of 1 mg/mL were prepared in methanol and stored at −20 °C. Further dilutions of these were prepared in acetonitrile and water by demand. Methanol was of HPLC grade. LC-MS grade acetonitrile was used for dilutions and as the eluent. All water was purified using an ELGA PURELAB Ultra water system (High Wycombe, UK). Analytical reagent grade formic acid (>98%) was used as an eluent additive. Deuterium oxide (Euriso-top) was used for the NMR analyses. The Fe-H-Beta-25-EIM catalyst was prepared by the evaporation impregnation method according to Saied et al. (2018) and the Cu-H-Beta-150-DP catalyst was prepared using the deposition-precipitation method according to Saeid et al. (submitted).

2.2. Ozonation experiments

The ozonation experiments were conducted according to Saeid et al. (2018). Briefly, the experiments were conducted in a double-jacketed glass reactor operating in a semi-batch mode. Gaseous ozone was produced by an ozone generator (Absolute Ozone, Nano model, Canada) using pure oxygen and nitrogen.

During the ozonation experiment, 1000 ml of deionized water was spiked with SDZ to give a final concentration of 10 mg/L. The reactor temperature was 25 °C.

Sulfadiazine and 2-aminopyrimidine quantification

For quantification, an aliquot (450 µL) of the samples were transferred to clean vials and 50 µL of water containing 1 µg/mL of the internal standard sulfadiazine-D_4 was added. A 12-point calibration curve of concentrations between 0.5 and 5000 ng/mL of SDZ and 2-aminopyrimidine was prepared in water. The internal standard method was used for the quantification. For LC-MS/MS analysis of SDZ and 2-aminopyrimidine, an Agilent 6460 triple quadrupole mass spectrometer equipped with an Agilent Jet Spray electrospray ionization (ESI) source was used in multiple reaction monitoring (MRM) mode. The mass spectrometric parameters are presented in supplementary information. The chromatographic separation was performed using an Agilent 1290 binary pump equipped with a vacuum degasser, an autosampler, a thermostatted column oven set to 30 °C, and a Waters xbrigde C18 column (2.1 × 50 mm, 3 µm). The eluents were 0.1% formic acid in water (A) and 0.1% formic acid in acetonitrile (B). Initially the composition was kept at 5 % (B) for 0.5 min, after which the composition was increased linearly to 95 % (B) over 4.5 min. The eluent composition was held at 95 % (B) for 0.5 min before being returned to the initial conditions over the next 0.1 min and given 1.4 min for equilibration. The flow rate was 0.4 ml/min and the injection volume was 10 µL.

2.3. Transformation product structure determination

For the structure determination, an Agilent 1100 LC/MSD ion trap mass spectrometer equipped with an electrospray ionization (ESI) source was used in full scan and MS^2 scan modes. The mass spectrometric parameters are presented in supplementary information. The chromatographic separation was conducted using an Agilent 1100 binary pump equipped with a vacuum degasser, an autosampler, a thermostatted column oven set to 30 °C, a Waters Atlantis T3 C18 column (2.1 × 100 mm, 3 µm) and a variable wavelength

detector set to 275 nm. The eluents were 0.1% formic acid in water (A) and 0.1% formic acid in acetonitrile (B). Initially the composition was kept at 0 % (B) for 5 min, after which the composition was increased linearly to 60 % (B) over a period of 19 min. The composition was further increased linearly to 95 % (B) over 1 min. The eluent composition was held at 95 % (B) for 4 min before being returned to the initial conditions over the next 1 min and given 10 min for equilibration. The flow rate was 0.3 ml/min and the injection volume was 30 µL.

High resolution mass spectra (HRMS) were obtained using a Bruker Daltonics micrOTOF quadrupole and time-of-flight mass spectrometer equipped with an electrospray ionization (ESI) source. The instrument was operated in full scan mode. Argon was used as drying gas and collision gas. The chromatographic separation was performed using an Agilent 1200 binary pump equipped with a vacuum degasser, an autosampler, a thermostatted column oven and a diode array detector. The column and chromatographic method was the same as above.

2.4. Semi-preparative HPLC

The main product according to the TIC chromatograms after 240 min of ozonation was isolated using semi-preparative HPLC. An aliquot of the ozonated sample (250 mL) was freeze dried and reconstituted in 1,5 mL of Milli-Q water.

For product isolation, an Agilent 1100 LC equipped with an analytical scale fraction collector was used. The chromatographic separation was performed using an Agilent 1100 quaternary pump equipped with a vacuum degasser, an autosampler, a thermostatted column oven set to 30 °C, a Thermo Hypersil-Keystone BDS C18 column (100 × 500 mm, 5 µm) and a diode array detector monitoring 254 nm. The method used for the HPLC is presented in supplementary information.

Pure fractions were combined and freeze dried. The residue was dissolved in 850 µL deuterium oxide and transferred to an NMR tube. The samples were analyzed using a 500 MHz Bruker AVANCE-III NMR-system.

2.5. Quantification of SDZ-P15

In order to quantify the amount of SDZ-P15 produced during the ozonation experiment, the purified SDZ-P8 was dissolved in 800 µL deuterium oxide and 2 mg maleic acid dissolved in 50 µL deuterium oxide was added as an internal standard. A quantitative NMR experiment was run to determine the ratio of product to internal standard. Subsequently a calibration curve of SZD-P15 was prepared by dissolving the sample in water. SDZ-P15 was quantified using HPLC. The method is presented in supplementary information.

3. Results and discussion

3.1. SDZ transformation kinetics

Non-catalytic transformation of SDZ

During the ozonation process, a mixture of oxygen and nitrogen is used as a feed gas. Higher oxygen levels lead to higher concentrations of ozone, however it also increases to cost of the process. The ozonator manufacturer suggested the use of a small amount of N_2 in the gas feed in order to enhance the performance of the generator. Three different nitrogen gas flow rates were investigated: 50 ml/min, 2.5 ml/min and 0 mL/min. The nitrogen flow velocity significantly affected the transformation of SDZ (Figure 1(a)). After five minutes of ozonation, 95 % of SDZ had been transformed at a nitrogen flow rate of 50 mL/min, whereas 99.9 % of SDZ had been transformed using no nitrogen flow at all. SDZ could no longer be detected after one minute at a nitrogen flow rate of 2.5 mL/min. Thus, a nitrogen flowrate of 2.5 mL/min is optimal for the transformation of SDZ.

178 The effect of the oxygen gas flow was investigated. The reaction was significantly slower when the oxygen
179 gas flow was decreased (Figure 1(b)). This is due to the lower concentration of ozone formed when the
180 oxygen gas flow is decreased. At oxygen flow rate of 202 mL/min, the concentration of SDZ decreased
181 below the level of quantification in 2 minutes, while only one minute was required to transform SDZ at a
182 flow rate of 445 mL/min. A higher gas flow rate enhances the transformation of SDZ, while also increasing
183 the cost of the process. The transformation of SDZ becomes drastically slower when the oxygen gas flow
184 rate is lower than 200 mL/min. Thus, a oxygen gas flow rate of at least 200 mL/min is recommended for
185 the ozonation of SDZ. When the flow rate was 0.034 L/min, the reaction order changed: initially the
186 reaction was of second order with an R^2 value of 0.991, but after 10 minutes, the reaction order changed
187 to a first order reaction with an R^2 value of 0.998. This indicated that the rate of the reaction was limited
188 by the amount of dissolved ozone.

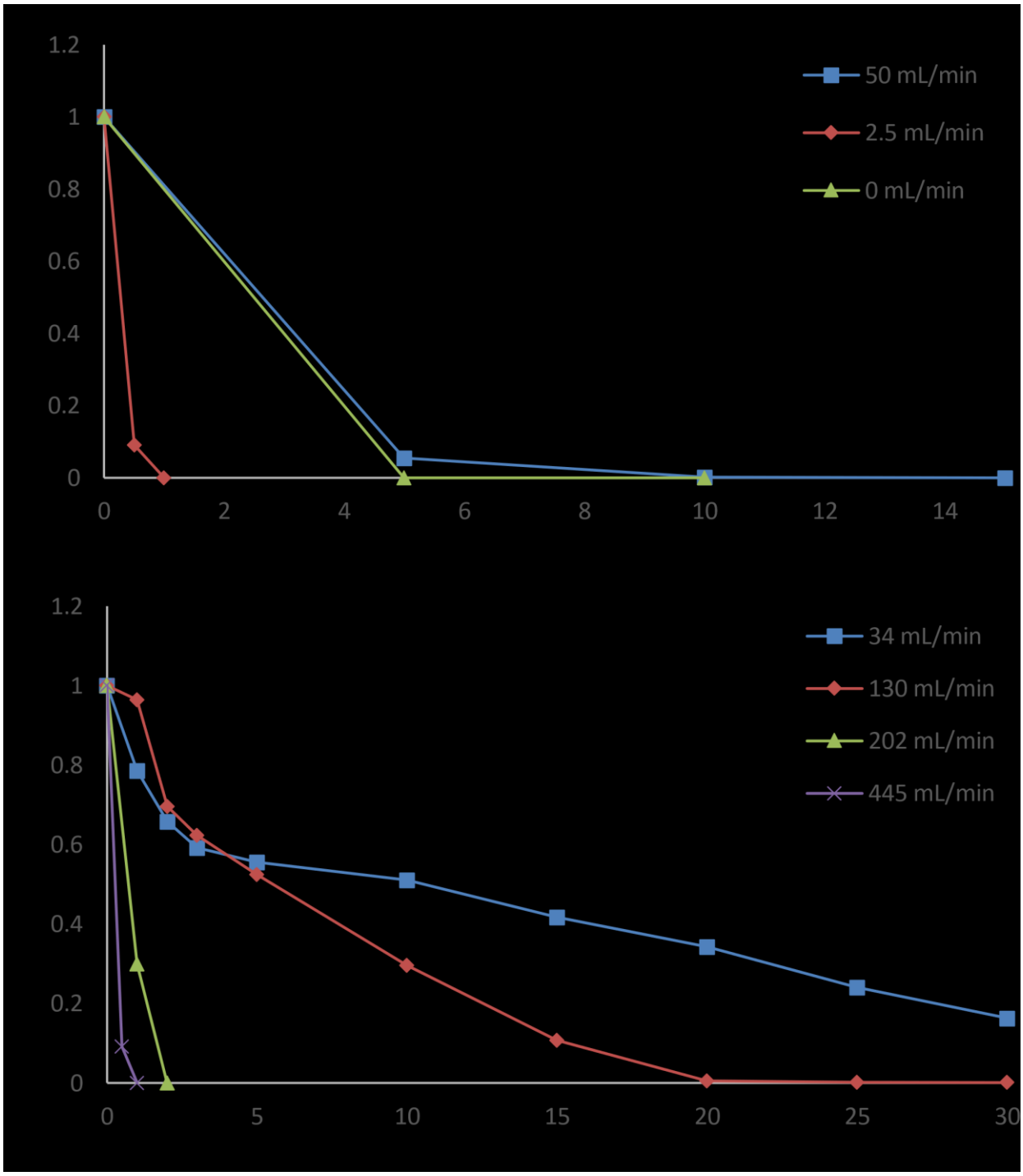

189

190 Figure 1. Transformation of SDZ with (a) different nitrogen flow rates and (b) different oxygen flow rates.

191 The numbers in the legend represent the gas flow rate.

192

Catalytic transformation of SDZ

The catalysts that were chosen for this work (Fe-H-Beta-25-EIM and Cu-H-Beta-150-DP) had previously been shown to enhance the transformation of the pharmaceuticals ibuprofen (IBU) and diclofenac (DCF). The Fe-H-Beta-25-EIM catalyst enhanced the transformation of the pharmaceutical due to the large amount of Brønsted and Lewis acid sites present on the catalyst (Saeid et al. 2018). The Cu-H-Beta-150-DP enhanced the transformation of the pharmaceutical due to the high concentration of metal in the catalyst (Saeid et al. 2019). The characterization of the catalysts has previously been published (Saeid et al. 2018, Saied et al. 2019). The presence of a catalyst does not affect the ozone concentration in the water. For this work, 0.5 g of catalysts were used. The transformation of SDZ depended partially on the catalyst used (figure 2). When the experiments were performed at the higher nitrogen flow fraction, the presence of the catalyst retarded the reaction. It was discovered that a lag time in the beginning of the experiment was affecting the kinetics when a catalyst was used. The concentration was more or less unchanged for the first five minutes before the concentration started to decrease. These results differ from the results obtained for IBU. Both catalysts enhanced the transformation of IBU, while they decreased the transformation of SDZ. This indicates the necessity of investigating the transformation of more than one pharmaceuticals for a catalyst. The difference between the effects of catalysts on the transformation of IBU and SDZ is due to the molecular structure of the different pharmaceuticals. IBU contains a carboxylic acid group, while SDZ does not. Instead, SDZ contains an amine group and a sulfonyl group. The increase in transformation rate observed when a catalyst is used in combination with ozone is considered to be due to the transformation of ozone into hydroxyl radicals, adsorption of organic to the catalyst followed by oxidation of dissolved ozone or adsorption of both ozone and organic molecules onto the catalyst followed by a surface reaction (Gomes et al. 2017). The enhancement of the transformation of IBU by catalytic ozonation is probably due to the adsorption of IBU to the catalyst surface. SDZ, on the other hand, does

not adsorb to the surface since there was no decrease in SDZ concentration during a 60-minute experiment where catalyst was used without ozonation.

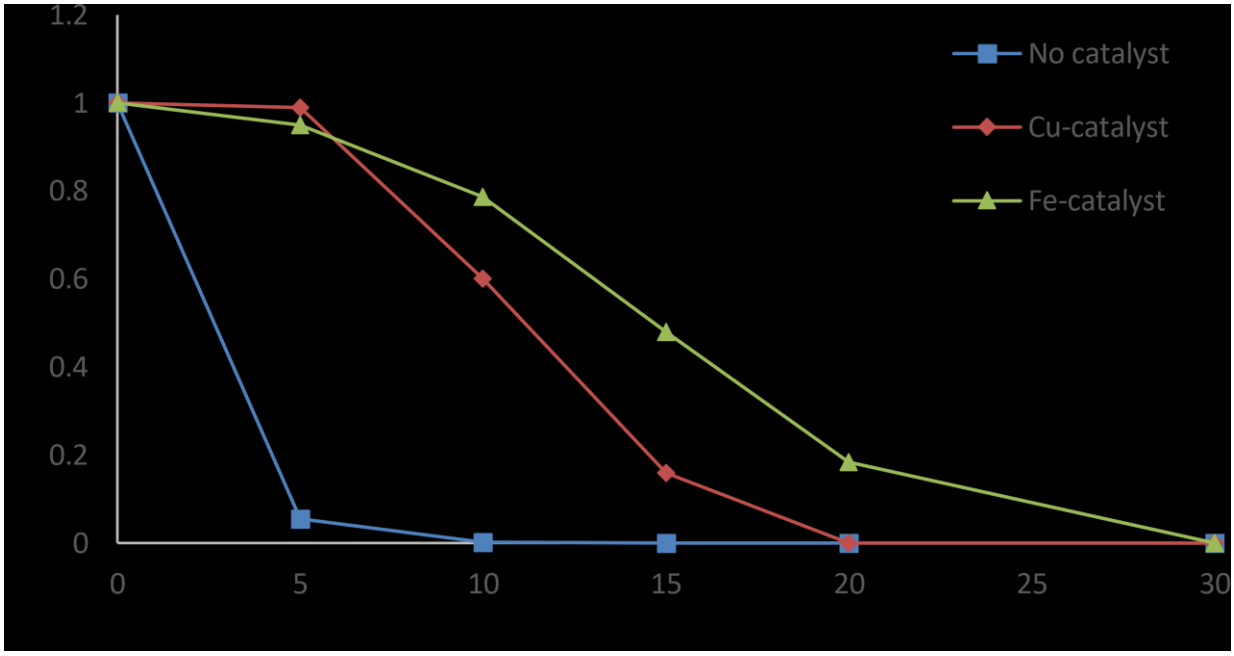

Figure 2. Catalytic and non-catalytic transformation of SDZ

3.2. SDZ transformation products

Some of the products identified in this study have previously been detected as SDZ transformation products, although none have been reported for ozonation processes. The product 2-aminopyrimidine (2-AP, Figure 3 (a), Table 1) is formed during several advanced oxidation processes (Wang et al. 2010; Rong et al. 2014; Guo et al. 2012; Fabiańska et al. 2014; Zou et al. 2014). Mono-hydroxylated products (SDZ-P1, Figure 3 (a), Table 1) have been reported as a product formed during phototransformation (Wang et al. 2010; Ma et al. 2015; Sukul et al. 2008) and electrochemical transformation (Rong et al. 2014; Fabiańska et al. 2014). SDZ-P3 (Figure 3 (a), Table 1) is formed during sonolysis (Zou et al. 2014) and phototransformation (Ma et al. 2015).

233 Table 1. SDZ and identified SDZ products

Compound	Proposed structure	m/z for $[M+H]^+$ peak	Fragment ions (m/z)	High resolution mass	Error (ppm)	Retention time (min)	Maximum EIC peak area compared to initial SDZ area
SDZ	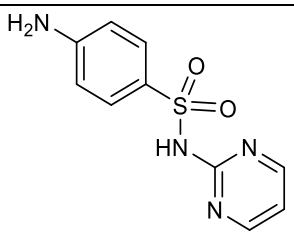	251	158, 156, 94, 92	-	-	14.6	-
2-AP	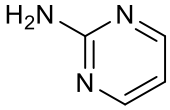	96	79,[a] 53,[a] 43[a]	-	-	2.2	1 %
SDZ-P1	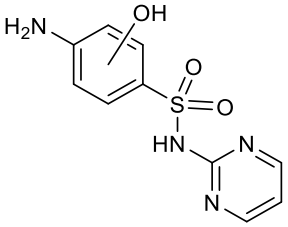	267	249, 203, 206, 158	-	-	11.5, 13.8	2 %
SDZ-P2	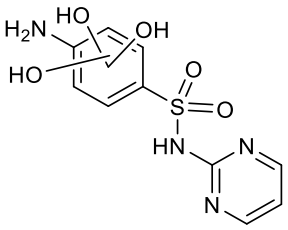	299	281, 263, 237	-	-	10.5, 12.2	<1 %
SDZ-P3	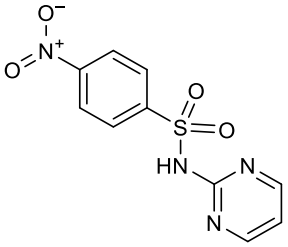	281	186, 140, 94	-	-	19.1	<1 %

SDZ-P4	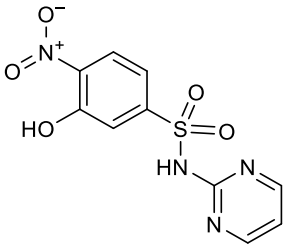	297	202, 158, 96	-	-	18.4	<1 %
SDZ-P5	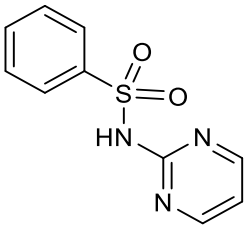	236	180, 141, 95, 77	-	-	18.1	1 %
SDZ-P6	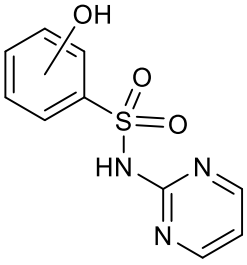	252	176, 158, 96	-	-	15.7	1 %
SDZ-P8	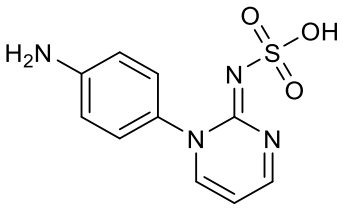	265[b]	187, 145, 170	-	-	2.4	<1 %
SDZ-P9	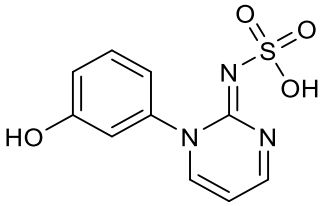	266[b]	188, 170	266.0209 188.0838	10 7.5	6.3	36 %
SDZ-P10	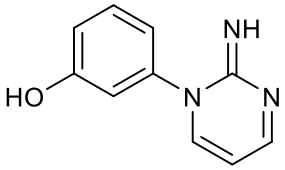	188	170	188.0824	0.1	15.5	8 %

SDZ-P11	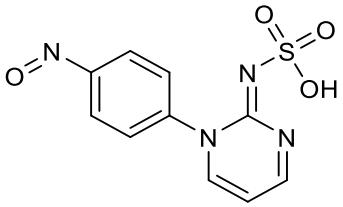	280	171, 188 252	-	-	3.9	<1 %
SDZ-P12	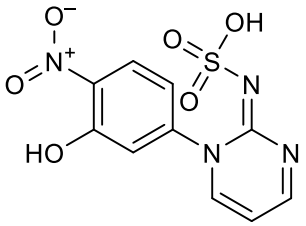	Not detected	233, 187, 204, 119	233.0679	1.9	4.6	25 %
SDZ-P13	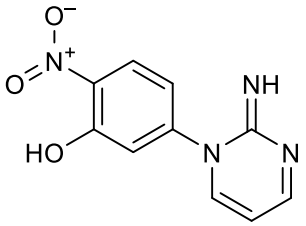	233	187, 215, 159	233.0641	14	22.5	7 %
SDZ-P14	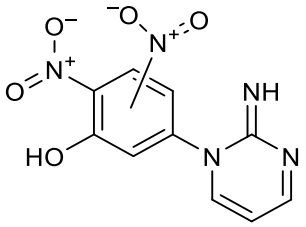	278 276[b]	260, 186, 172, 158	276.0346[b]	8.3	24.3	1 %
SDZ-P15	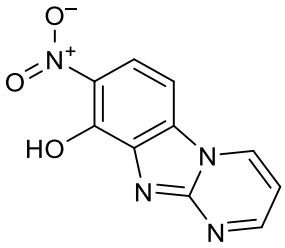	231	213, 169, 158, 130	231.0522	1.7	15.0 17.3	49 % 1 %
				231.0512	2.7	17.9	13 %
SDZ-P16	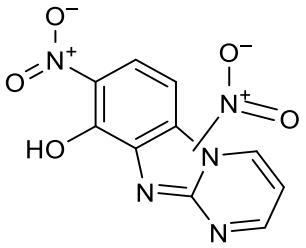	276	230, 214, 156	276.0375	2.2	16.2	3 %

SDZ-P17	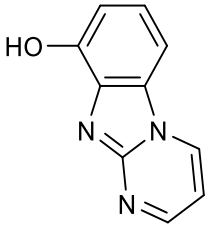	186	159, 169, 131	186.0649	9.9	12.9	16 %

a. Results from QqQ, no fragments detected with ion trap.

b. $[M-H]^-$ peak

3.3. N-(pyrimidin-2-yl) benzenesulfonamide products

In this study, two isomers of SDZ-P1 were detected. They were distinguished by their different retention times: 11.5 min and 13.8 min. Both isomers have a fragment peak with m/z 158, indicating that the pyrimidine ring was unchanged. An OH group had consequently been attached to the aniline ring.

Two isomers of SDZ-P2 were formed when three hydroxyl groups were added to SDZ. None of the characteristic SDZ fragments were present, which indicates that both aromatic rings had been hydroxylated.

SDZ-P4 had $[M+H]^+ = 297$. MS^2 scans show a fragment ion at m/z 158, indicating that the transformations have taken place on the aniline ring. SDZ-P4 were suggested to be formed via the oxidation of the amine to a nitro group and the addition of an OH group to the aromatic ring.

SDZ-P5 had $[M+H]^+ = 236$ and a fragment ions at m/z =95, which corresponds to the pyrimidine ring. The aniline peaks at m/z = 156 and 94 was not observed. Instead there were peaks at m/z = 77 and 141. This indicated that the NH_2 group of the aniline ring had been removed. SDZ-P5 was probably formed from a radical reaction of SDZ similar to the one Chignell et al noted for the photolytic cleavage of sulfanilamide (2008).[23]

252 The product SDZ-P6 showed $[M+H]^+$ = 252, compared to SDZ with $[M+H]^+$ = 251. Because of this and the
253 similarities of the mass spectra for the two compounds, the structure of SDZ-P6 was suggested to be SDZ
254 where the NH_2 group had been replaced by an OH group. This product could be formed via hydroxylation
255 of SDZ-P5.

256 Based on the identified products some pathways for the first transformation of SDZ are presented in Figure
257 3 (a). SDZ was transformed via the addition of one or more hydroxyl group, the oxidation of the amine
258 group to a nitro group, the cleavage of the S-N bond and the elimination of the amine group followed by
259 an addition of a hydroxyl group.

260

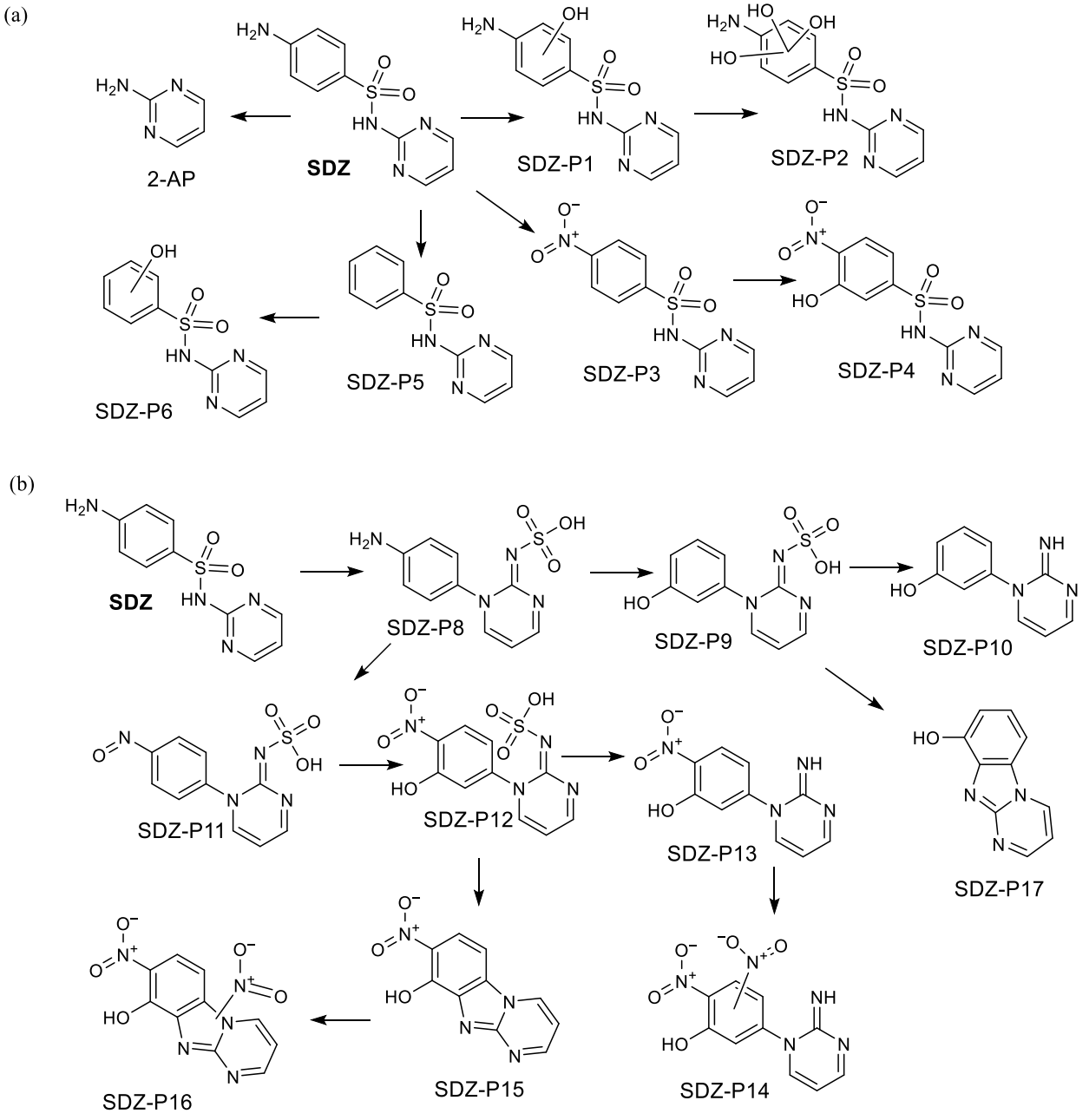

Figure 3. SDZ ozonation pathways (a) the N-(pyrimidin-2-yl) benzenesulfonamide pathway and (b) the rearrangement pathway

3.4. SDZ rearrangement products

When Sulfadiazine is ozonated the compound undergoes a rearrangement reaction (Figure S3). The rearrangement involves the formation of a new bond between the nitrogen atom in the pyrimidine ring and the aniline ring as well as breaking the bond between the sulfonyl group and the aniline ring and the addition of a hydroxyl group to the sulfonyl group to form a sulfonic acid group. This leads to the formation of product SDZ-P8 (Figure 3 (b) and Table 1) (Gao et al. 2012).[16] The rearrangement mechanism has been studied by Gao et al.[16] and Tentscher et al (Gao 2012, Tentscher 2013) .[22] Both groups propose that the rearrangement takes place via a Smiles type rearrangement reaction (Figure S3) and that the reactions involves the formation of a radical.

The retention time of SDZ-P8 was 2.4 min. This indicates that SDZ-P8 was more polar than SDZ (RT 14.6 min). This is due to the presence of the sulfonilic acid group. SDZ-P8 had $[M-H]^-$ = 265. The positive mass spectrum of SDZ-P8 did not show the $[M+H]^+$ peak. Instead the base peak of the spectrum was m/z = 187, i.e. the sulfonic acid group was cleaved off in the ion source and two protons were added. The main fragments of SDZ-P1 in positive mode were m/z 170, corresponding to the loss of the amine group and 145 corresponding to the loss of a CN_2 fragment.

SDZ-P9 was $[M-H]^-$ = 266. In positive mode the $[M+H]^+$ peak could not be detected, instead the highest positive fragment ion was m/z = 188. The fragmentation pattern of SDZ-P9 was almost identical to the fragmentation pattern of SDZ-P8, however the base peak of SDZ-P9 was one mass unit higher than SDZ-P8. The main fragment of SDZ-P9 was m/z = 170, indicating the loss of an OH group. The positive high resolution mass of SDZ-P9 gave the elemental elemental formula $C_{10}H_{10}N_3O$ (error 7.5 ppm) in positive mode and $C_{10}H_8N_3O_4S$ (error 10 ppm) in negative mode. SDZ-P9 seemed to be formed via the cleavage of

287 the bond between the NH_2 group and the aromatic ring and the addition of an OH group (Figure 3 (b),
288 Table 1).

289 SDZ-P10 had $[M+H]^+$ = 188. SDZ-P10 had the elemental formula $C_{10}H_{10}N_3O$ (error of 0.1 ppm). SDZ-P10 was
290 formed by the loss of the sulfonic acid group from SDZ-P9 (Figure 3 (b), Table 1).

291 SDZ-P11 had the $[M+H]^+$ peak 280 and the retention time 3.8 minutes. SDZ-P11 was likely formed when
292 the NH_2 group of SDZ-P8 was oxidized to an NO group (Figure 3 (b), Table 1).

293 SDZ-P12 had a positive base peak value at m/z = 233. Its retention time was 4.6 min, indicating that the
294 SO_3 group was still attached, even though no peak with m/z = 311 could be detected in negative mode.
295 The main fragments of SDZ-P12 were m/z at 187, corresponding to the loss of an NO_2 group and m/z at
296 216 corresponding to the loss of an OH group. The positive HRMS of SDZ-P12 gave the elemental formula
297 $C_{10}H_9N_4O_3$ (error 1.9 ppm). This indicated that the NH_2 group of SDZ-P8 had been oxidized to an NO_2 group
298 and that an OH group had been added (Figure 3 (b), Table 1).

299 SDZ-P13 had $[M+H]^+$ = 233 and the HRMS gave the elemental formula $C_{10}H_9N_4O_3$ (error 14 ppm). SDZ-P13
300 had RT = 22.5 min, indicating that this was a less polar compound than SDZ. The structures for SDZ-P12
301 and SDZ-P13 were similar, except SDZ-P13 did not contain a sulfanilic acid group (Figure 3 (b), Table 1).

302 SDZ-P14 had $[M+H]^+$ = 278. The negative HRMS of SDZ-P2 gave the elemental formula $C_{10}H_6N_5O_5$ (error 8.3
303 ppm). This product was formed via the addition of an NO_2 group to SDZ-P13 (Figure 3 (b), Table 1). In
304 experiments with a high nitrogen flow nitric acid was formed from the ozonation of N_2. Nitric acid may
305 react with aromatic compounds through an electrophilic substitution reactions.

306 SDZ-P15 had $[M+H]^+$ = 231. The positive HRMS of SDZ-P2 gave the elemental formula $C_{10}H_7N_4O_3$ (error 1.7
307 ppm). The main fragments were 213 (loss of an OH group), and 169 (loss of an NO_2 group). SDZ-P15 was
308 formed via the loss of the SO_3 group and the addition of an OH group to SDZ-P15 and the oxidation of the

309 NH_2 group to an NO_2 group. Additionally, two protons, one from the aniline ring and one from the NH group
310 on the pyrimidine ring seemed to have been lost from SDZ-P15. This indicates a ring closing joining the NH
311 group from the pyrimidine ring to the aniline ring (Figure 3 (b), Table 1).

312 SDZ-P15 was the major product present at the end of the experiments (Figure 4 (a)). In order to further
313 elucidate the structure of SDZ-P15 a sample taken from the reaction mixture at 240 minutes of ozonation.
314 After lyophilization SDZ-P15 was isolated using semi-preparative HPLC. It was noted that SDZ-P15 had a
315 yellow color and thus it was most likely that SDZ-P15 was the product responsible for the color change
316 observed in the experiment. The structure of SDZ-P15 was determined by NMR.

317 The ^{1}HNMR spectrum of SDZ-P15 shows a singlet at a shift of 8.4 which corresponded to 0.6 H when the
318 sample was first analyzed and 0.4 H when the sample was re-analyzed after being stored in D_2O for two
319 months. This peak is characteristic of an OH or NH_2 peak. The presence of a peak for an OH or NH2 group
320 in a spectrum run in D_2O indicates that the proton could not be easily exchanged. The peak could be the
321 proton OH group involved in a strong intramolecular hydrogen bond with the adjacent NO_2 group. The two
322 protons on the aniline ring were probably in ortho position to each other since the coupling constant
323 between them was 9 Hz and no other couplings were detected.

324 In addition, two isomers of SDZ-P15 were observed with LC-MS. The isomers probably have OH group was
325 in different positions compared to SDZ-P15.

326 SDZ-P16 had a similar MS^2 mass spectrum and retention time to SDZ-P15. The HRMS of SDZ-P16 gave the
327 elemental formula $C_{10}H_6N_5O_5$ (error 2.2 ppm). This indicates that SDZ-P16 was formed from SDZ-P15 by
328 addition of an NO_2 group (Figure 3 (b), Table 1).

329 Also the product SDZ-P17 seemed to be formed via a ring closing of a SDZ rearrangement product. This
330 product had $[M+H]^+ = 186$. The HRMS of SDZ-P17 gave the elemental formula $C_{10}H_8N_3O$ (error 9.9 ppm).

The fragmentation of SDZ-P17 was similar to that of SDZ-P15. This indicated that SDZ-P17 was similar to that of SDZ-P15, except that SDZ-P17 did not have an NO_2 group. Since the main isomer of SDZ-P15 had the OH group ortho to the NO_2 group, it is likely that SDZ-P17 had the OH group in the same position (Figure 3 (b), Table 1).

SDZ-P15 could be formed from either SDZ-P12 or SDZ-P13. Figure 4 (a) shows the peak areas for the extracted ion chromatograms for SDZ-P12, SDZ-P13 and SDZ-P15 with SDZ for comparison. The concentration of SDZ-P15 continued to increase after SDZ-P13 was no longer detected. Because of this, it seems more likely that SDZ-P15 was formed from SDZ-P12, i.e. the product that had the SO_3 group still attached. The mechanism of this reaction is unknown, however a ring-closing of a similar structure has been proposed for the pesticide pyrimethanil (Aziz et al. 2013).[23] The mechanism most likely involves a radical reaction. It is likely that the SO_3 group acts as a leaving group and that the hydroxyl group is involved in the formation of SDZ-P13.

Based on this and the above results the transformation pathway of SDZ is presented in Figure 3 (b). The mechanism presented here is similar, but more extensive compared to previously reported mechanisms. Previously published mechanisms for the formation of SDZ oxidation products involve reactions with hydroxyl radicals to form smaller degradation products such as 2-AP (Neafsey et al. 2010), hydroxylated SDZ products (Wang et al. 2010). The transfer of a single electron from a suitable oxidant leading to rearrangement and SO_2 extrusion (Tentscher at al. 2013). When sulfate radicals are used as oxidizing agents, smaller degradation products and a rearrangement product are formed (Feng et al. 2016).

Not only the structure, but also the toxicity of the formed products is of interest. A full study if the toxicity of the products is beyond the scope of this work, however the toxicities of the main products were estimated with the ECOSAR software. The results of these calculations are presented in the

supporting material. Generally, the rearrangement products, are more toxic than SDZ, indicating the need to optimize the zonation process in order to reduce the formation of rearrangement products.

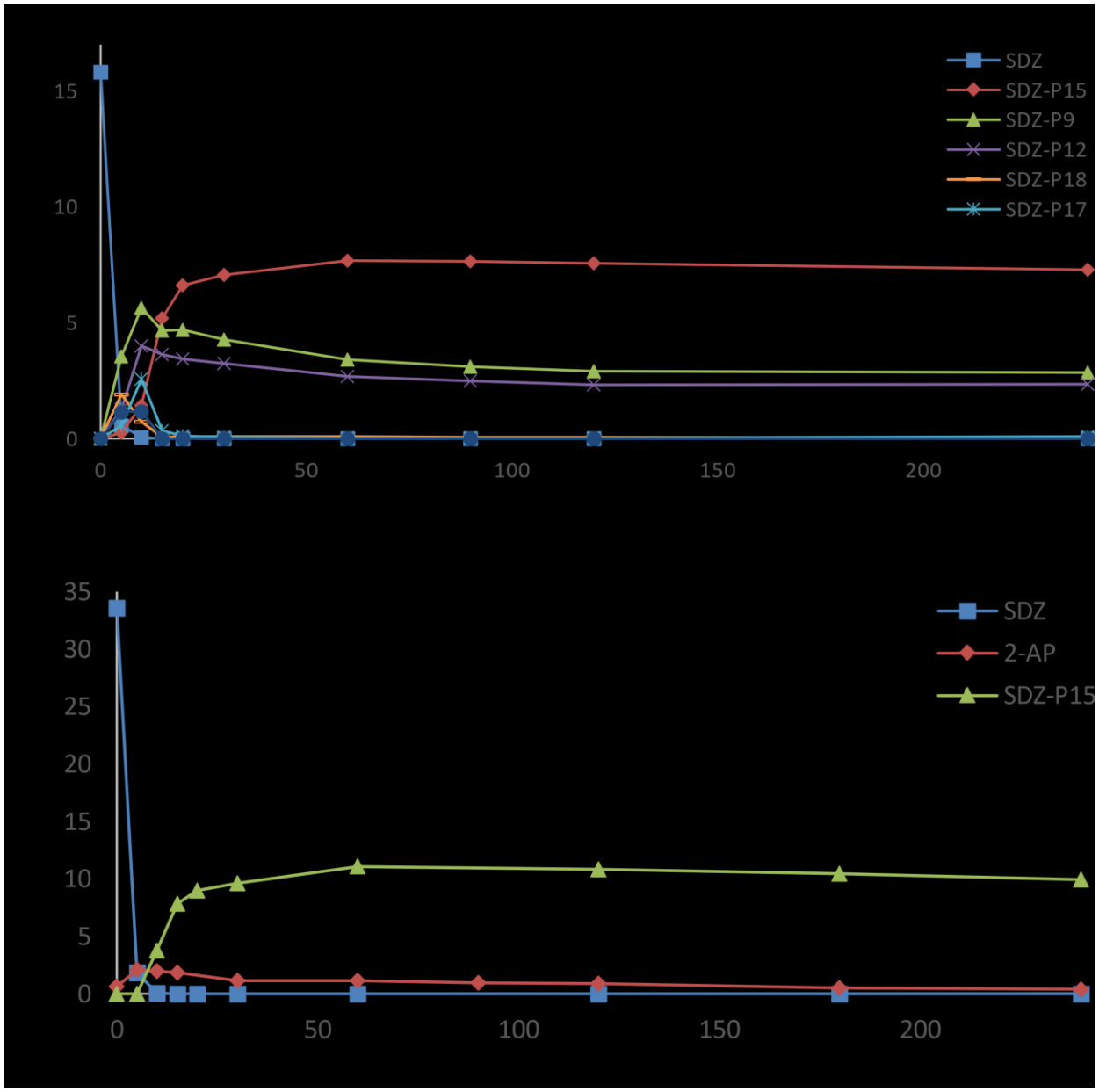

Figure 4. (a) Extracted ion chromatogram peak areas for SDZ and its major products and (b) molar concentration of SDZ, and products 2-AP and SDZ-P15.

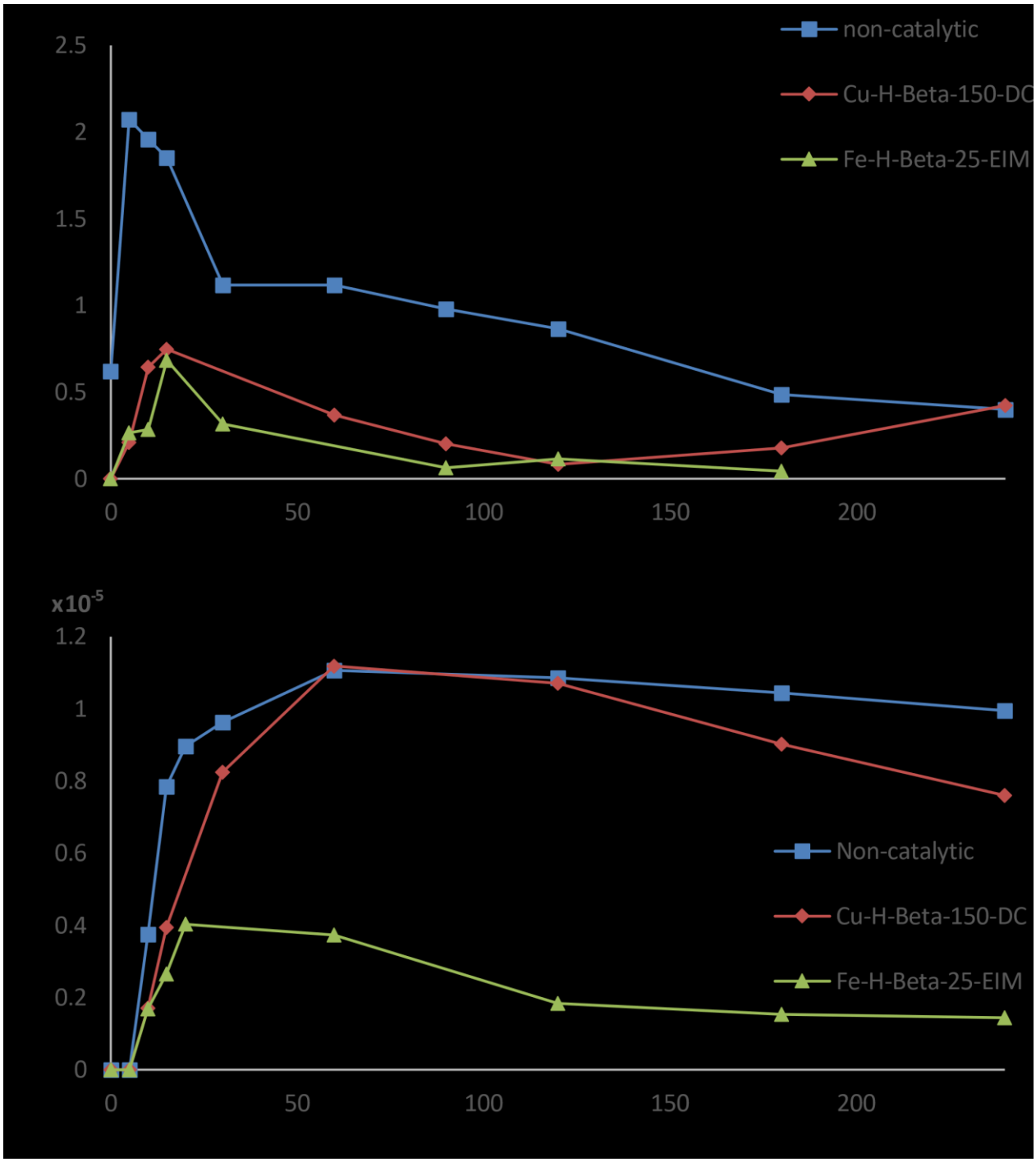

358

359 Figure 5. (a) Concentration of 2-AP formed during catalytic and non-catalytic transformation of SDZ (b)
360 Concentration of SDZ-P15 formed during catalytic and non-catalytic transformation of SDZ.

361

362

3.5. Quantification of SDZ products

The commercially available 2-AP was purchased, and a method was developed to quantify the product with QqQ MS. Around 0.2 mg/L (or 2 µM) 2-AP was formed in both high and low nitrogen conditions, which corresponds to 6 % of the original SDZ amount. Under high nitrogen flow conditions, the concentration of 2-AP increased to a maximum in 5 minutes and low nitrogen flow conditions the maximum concentration of 2-aminopyrimidine appeared at 10 min. The transformation of 2-AP was slow compared to SDZ: after 240 min 0.04 mg/L 2-AP was detected (Figure 4 (b)). During catalytic transformation of SDZ, less 2-AP was formed than during non-catalytic transformation (Figure 5 (a)). This is probably due to the slower transformation of SDZ during catalytic ozonation.

The concentration of SDZ-P15 as a function of time in the ozonation experiment can be seen in figure 4 (b). The concentration increased to a maximum at 60 minutes after which the concentration started to decrease. The maximum concentration of SDZ-P8 was 1.1 $x10^{-5}$ mol/L. The initial concentration of SDZ was 4 $x10^{-5}$ mol/L. This means that 28 % of SDZ was transformed into SDZ-P15. The same concentration of SDZ-P15 was formed when Cu-H-Beta-150-DP was used as a catalyst, while significantly less SDZ-P15 was formed when Fe-H-Beta-25-EIM was used as a catalyst. This indicates that when Fe-H-Beta-25-EIM enhances the transformation of this product. This is beneficial since SDZ-P15 is significantly more stable than SDZ, so while the presence of the catalyst does not enhance the transformation of SDZ. Instead it enhances the transformation of the major product formed during the ozonation process. Catalysts have previously been shown to enhance the removal of pharmaceutical transformation product even when the catalyst did not affect the transformation of the parent compound (Gomes et al. 2017). Thus, a catalyst can enhance the complete removal of SDZ from wastewater.

Other major products during the ozonation process were SDZ-P9, SDZ-P12, and SDZ-P17. Figure 4 (a) shows the EIC peak areas for SDZ and the major products. Three of the products, SDZ-P9, SDZ-P12 and SDZ-P15

were significantly more stable towards ozonation than SDZ and could still be detected after 240 min of ozonation. The EIC peak areas for the products were similar for both the catalytic and non-catalytic experiments.

The concentration of the rearrangement products were estimated by comparing the maximum EIC peak area of the product to the initial EIC peak area for SDZ (Table 1). The error with this method was high. E.g., the maximum peak area of SDZ-P15 was 49 % of the initial peak area of SDZ, while the actual concentration was 28 %.

4. Conclusions

SDZ was readily transformed in ozonation reactions. The most efficient elimination took place when the nitrogen flow rate was 0.0025 L/min and the oxygen flow rate was 445 mL/min. Under these conditions, SDZ was transformed in less than one minute. The catalysts did not enhance the transformation of SDZ.

The products that were formed depended on the reaction conditions. The presence of a catalyst did not influence which products were formed; however id did affect the concentration of some of the products. Two of the products, 2-AP and SDZ-P15 were quantified. SDZ-P15 is the major product, 28 % of SDZ transformed into SDZ-P15. The Cu-H-Beta-150-DP catalyst did not affect the formation of SDZ-P15, while significantly less SDZ-P15 was formed when Fe-H-Beta-25-EIM was used. A small amount (6 %) of SDZ is transformed into 2-AP. The concentration of 2-AP was lower when a catalyst was used compared to non-catalytic experiments.

SDZ is transformed by two different pathways during ozonation reactions. One pathway involves the addition of one or more hydroxyl group, the oxidation of the amine group to a nitro group and the elimination of the amine group followed by an addition of a hydroxyl group. The other pathway involves a

rearrangement of SDZ followed by addition of OH groups, loss of the SO_2 group, addition of an NO_2 group and a ring-closing reaction. The pathway involving rearrangement seems to be the dominant pathways in the ozonation of SDZ, according to the UV and EIC peak areas of the chromatograms. Many of the products formed are more stable than SDZ and can still be detected at the end of the experiment.

References

Aziz, K, Ahmad, R, Sophie, B, Farouk, J, Bouchonnet, S (2013) Structural characterization of photoproducts of pyrimethanil. J. Mass Spectrom. 48: 983-987

Baquero, F, Martínez, J, Cantón, R (2008) Antibiotics and antibiotic resistance in water environments. Curr. Opin. Biotech. 19: 260-265

Boreen, A, Arnold, W, McNeill, K (2005) Triplet-Sensitized Photodegradation of Sulfa Drugs Containing Six-Membered Heterocyclic Groups: Identification of an SO2 Extrusion Photoproduct. Environ. Sci. Technol. 39: 3630-3638

Chignell, C. F, Kalyanaraman B, Mason, R. P, Sik, R. H (2008) Spectroscopic studies of cutaneous photosensitizing agents—I. Spin trapping of photolysis products from sulfanilamide, 4-aminobenzoic acid and related compounds. Photochem. Photobiol. 32: 563-571

Donner, E, Kosjek, T, Qualmann, S, Kusk, K. O, Heath, E, Revitt, D. M, Ledin, A, Andersen, H. R (2013) Ecotoxicity of carbamazepine and its UV photolysis transformation products. Sci. Total Environ. 443: 870-876

428 Fabiańska, A, Białk-Bielińska, A, Stepnowski, P, Stolte, S, Siedlecka, E. M (2014) Electrochemical degradation
429 of sulfonamides at BDD electrode: Kinetics, reaction pathway and eco-toxicity evaluation. J. Hazard. Mater.
430 280: 579-587

431 Fatta-Kassinos, D, Meric, S, Nikolaou, A (2011) Pharmaceutical residues in environmental waters and
432 wastewater: current state of knowledge and future research. Anal. Bioanal. Chem. 399: 251-275

433 Feng, Y, Wu, D, Deng, Y, Zhang, T, Shih, K (2016) Sulfate radical-mediated degradation of sulfadiazine by
434 $CuFeO_2$ rhombohedral crystal-catalyzed peroxymonosulfate: synergistic effects and mechanisms Env. Sci.
435 Technol. 50: 3119-3127

436 Gao, J, Hedman, C, Liu, C, Guo, T, Pedersen, J (2012) Transformation of Sulfamethazine by Manganese Oxide
437 in Aqueous Solution. Environ. Sci. Technol. 46: 2642-2651

438 Gao, G, Kang, J, Shen, J, Chen, Z, Chu, W (2016) Catalytic ozonation of sulfamethoxazole by composite iron-
439 maganese silicate oxide: cooperation mechanism between adsorption and catalytic reaction. Environ. Sci.
440 Pollut. R. 23: 21360-21368

441 Garoma, T, Umamaheshwar, S. K, Mumper, A (2010) Removal of sulfadiazine, sulfamethizole,
442 sulfamethoxazole, and sulfathiazole from aqueous solution by ozonation. Chemosphere 79: 814-820

443 Gomes, J, Costa, R, Quinta-Ferreira, R, Martins, R (2017) Application of ozonation for pharmaceuticals
444 and personal care products removal from water, Sci. Total Environ. 586: 265–283

445 Guo, Z, Zhou, F, Zhao, Y, Zhang, C, Liu, C, Bao, C, Lin, M (2012) Gamma irradiation-induced sulfadiazine
446 degradation and its removal mechanisms. Chem. Eng. J. 191: 256-262

447 Hong, C, JianYing, H, LeZhen, W, Bing, S (2008) Occurrence of sulfonamide antibiotics in sewage
448 treatment plants, Chin. Sci. Bull. 53: 514-520

449 Kosjek, T, Heath, E (2008) Applications of mass spectrometry to identifying pharmaceutical transformation
450 products in water treatment. Trends Anal. Chem. 27: 807-820

451 Kümmerer, K (2004) Resistance in the environment. J. Antimicrob. Chemoth. 54: 311-320

452 Li, G, Ben, W, Ye, H, Zhang, D, Qiang, Z (2018) Performance of ozonation and biological activated carbon in
453 eliminating sulfonamides and sulfonamide-resistant bacteria: A pilot-scale study. Chem. Eng. J. 341: 327-
454 334.

455 Li, W (2014) Occurrence, sources, and fate of pharmaceuticals in aquatic environment and soil. Environ.
456 Pollut. 187: 193-201

457 Liu F, Ying, G-G, Tao, R, Zhao, J-J, Yang, J-F, Zhao, L-F (2009) Effects of six selected antibiotics on plant
458 growth and soil microbial and enzymatic activities. Environ. Pollut. 157: 1636-1642

459 Ma, Y, Zhang, K, Li, C, Zhang, T, Gao, N (2015) Oxidation of Sulfonamides in Aqueous Solution by UV-TiO2-
460 Fe(VI). BioMed Res Int http://dx.doi.org/10.1155/2015/973942

461 McDowell, D, Huber, M, Wagner, M, von Gunten, U, Ternes, T (2005) Ozonation of Carbamazepine in
462 Drinking Water: Identification and Kinetic Study of Major Oxidation Products. Environ. Sci. Technol. 39:
463 8014-8022

464 Meierjohann, A, Kortesmäki, E, Brozinski, J-M, Kronberg, L (2017) An online SPE LC-MS/MS method for
465 the analysis of antibiotics in environmental water. Environ. Sci. Pollut. Res. 24: 8693-8699

466 Michael, I, Rizzo, L, McArdell, C. S, Manaia, C. M, Merlin, C, Schwartz, T, Dagot, C, Fatta-Kassinos, D (2013)
467 Urban wastewater treatment plants as hotspots for the release of antibiotics in the environment: A review
468 Water Res. 47: 957-995

469 Nasuhoglu, D, Yargeau, V, Berk, D. Photo-removal of sulfamethoxazole (SMX) by photolytic and
470 photocatalytic processes in a batch reactor under UV-C radiation (λmax=254nm) (2011) J. Hazard. Mater.
471 186: 67-75

472 Nawrocki, J, Kasprzyk-Hordern (2010) The efficiency and mechanisms of catalytic ozonation Appl. Catal. B:
473 Environ. 99: 27-42

474 Neafsey, K, Zeng, X, Lemley, A (2010) Degradation of Sulfonamides in Aqueous Solution by Membrane
475 Anodic Fenton Treatment. J. Agric. Food Chem. 58: 1068-1076

476 Pal, A, Gin, K, Lin, A, Reinhard, M (2010) Impacts of emerging organic contaminants on freshwater
477 resources: Review of recent occurrences, sources, fate and effects. Sci. Total Environ. 408: 6062-6069

478 Rong, S, Sun, Y, Zhao, Z (2014) Degradation of sulfadiazine antibiotics by water falling film dielectric barrier
479 discharge. Chinese Chem. Lett. 25: 187-192

480 Saeid, S, Tolvanen, P, Kumar, N, Eränen, K, Peltonen, J, Peurla, M, Mikkola, J-P, Franz, A, Salmi, T (2018)
481 Advanced oxidation process for the removal of ibuprofen from aqueous solution: A non-catalytic and
482 catalytic ozonation study in a semi-batch reactor. Appl. Cat. B 230: 77-90

483 Saeid, S, Kråkström, M, Tolvanen, P, Kumar, N, Eränen, K, Peltonen, J, Peurla, M, Mikkola, J-P, Maël, L,
484 Kronberg, L, Eklund, P, Salmi, T (submitted) Removal of ibuprofen from aqueous solution using combination
485 of heterogeneous catalysts and ozone: Effect of catalysts synthesis, metal particle size, acid sites and
486 structure of supports

487 Sui, M, Xing, S, Zhu, C, Sheng, L, Lu, K, Gao, N (2011) Kinetics of Ozonation of Typical Sulfonamides in Water.
488 Biomed. Environ. Sci. 24: 255-260

Sukul, P, Lamshöft, M, Zühlke, s, Spiteller, M (2008) Photolysis of ^{14}C-sulfadiazine in water and manure Chemosphere 71: 717-725

Tentscher, P, Eustis, S, Kristopher, M, Samuel, A (2013) Aqueous Oxidation of Sulfonamide Antibiotics: Aromatic Nucleophilic Substitution of an Aniline Radical Cation. Chem. Eur. J. 19: 11216-11223

Wang, W, Wu, Q, Huang, N, Xu, Z, Lee, M, Hu, H (2018) Potential risks from UV/H2O2 oxidation and UV photocatalysis: A review of toxic, assimilable, and sensory-unpleasant transformation products. Water Res. 141: 109-125

Wang, Y, Liang, J, Liao, X, Wang, L-S, Loh, T, Dai, J, Ho, Y (2010) Photodegradation of Sufadiazine by Geothite-oxalate suspension under UV light irradiation. Ind. Eng. Chem. Res. 46: 3527-3532

Wei, R, Ge, F, Huang, S, Chen, M, Wang, R (2010) Occurrence of veterinary antibiotics in animal wastewater and surface wateraround farms in Jiangsu Province, China. Chemosphere 82: 1408-1414

Witte, W (1998) Medical Consequences of Antibiotic Use in Agriculture. Science 279: 996-997

Yang, J, Yang, L, Ying, G, Liu, C, Zheng, L, Luo, S (2017) Reaction of antibiotic sulfadiazine with manganese dioxide in aqueous phase: Kinetics, pathways and toxicity assessment. J. Environ. Sci. Heal. A 52: 135-143

Yang, S, Lin, C, Wu, C, Ng, K, Yu-Chen Lin, A, Andy Hong, P (2012) Fate of sulfonamide antibiotics in contact with activated sludge – Sorption and biodegradation. Water Res. 46: 1301-1308

Zhou, T, Zou, X, Mao, J, Wu, X (2016) Decomposition of sulfadiazine in a sonochemical Fe0-catalyzed persulfate system: Parameters optimizing and interferences of wastewater matrix. Appl. Catal. B- Environ. 185: 31-41

Zou, X, Zhou, T, Mao, J, Wu, X (2014) Synergistic degradation of antibiotic sulfadiazine in a heterogeneous ultrasound-enhanced Fe0/persulfate Fenton-like system. Chem. Eng. J. 257: 36-44